Brief Communications

Estimate of the Chloride Concentration in a Central Glutamatergic Terminal: A Gramicidin Perforated-Patch Study on the Calyx of Held

Gareth D. Price and Laurence O. Trussell
Oregon Hearing Research Center, Vollum Institute, Oregon Health and Science University, Portland, Oregon 97239

The function of presynaptic terminals is regulated by intracellular Cl^-, the levels of which modify vesicular endocytosis and transmitter refilling and mediate the effects of presynaptic ligand-gated Cl^- channels. Nevertheless, the concentration of Cl^- in a central nerve terminal is unknown, and it is unclear whether terminals can regulate Cl^- independently of the soma. Using perforated-patch recording in a mammalian synapse, we found that terminals accumulate Cl^- up to 21 mM, between four and five times higher than in their parent cell bodies. Changing $[Cl^-]$ did not alter vesicular glutamate content in intact terminals, unlike *in vitro* experiments. Thus, glutamatergic terminals maintain an elevated Cl^- concentration without compromising synaptic transmission.

Key words: **chloride; perforated-patch; calyx of Held; auditory; glycinergic; KCC2**

Introduction

The release and recycling of glutamate at nerve terminals is influenced, directly or indirectly, by the cytosolic chloride concentration ($[Cl^-]_i$). Activation of presynaptic Cl^--permeable GABA or glycine receptors depolarizes terminals, leading to inhibition (Saridaki et al., 1989; Zhang and Jackson, 1993; Rudomin and Schmidt, 1999) or facilitation (Jang et al., 2001, 2006; Turecek and Trussell, 2001) of transmitter release; evidence suggests that the polarity of modulation depends on the amount of depolarization, which is partly determined by $[Cl^-]_i$. *In vitro* biochemical experiments have shown that glutamate loading into synaptic vesicles is stimulated by low $[Cl^-]$ (~4–10 mM) and inhibited by $[Cl^-] > \sim 20$ mM (Naito and Ueda, 1985; Tabb et al., 1992; Takamori et al., 2000; Varoqui et al., 2002). Finally, changes in $[Cl^-]_i$ may also affect the rate of endocytosis (Hull and von Gersdorff, 2004).

Although these observations suggest a need for tight regulation of $[Cl^-]_i$, it is unclear whether a terminal can regulate Cl^- independently of its soma. There is little difference between somatic and terminal $[Cl^-]$ in retinal bipolar cells (Billups and Attwell, 2002; Duebel et al., 2006); likewise $[Cl^-]$ is elevated similarly in dorsal root ganglion (DRG) terminals (Rudomin and Schmidt, 1999) as in DRG soma (Nishi et al., 1974; Alvarez-Leefmans et al., 1988). We measured $[Cl^-]_i$ in the calyx of Held, a giant glutamatergic terminal in the auditory brainstem and found that the terminal accumulated Cl^- whereas the parent cell body extruded it. We also studied the effect of the presynaptic $[Cl^-]$ on miniature EPSC (mEPSC) amplitudes and conclude that altering $[Cl^-]_i$ does not modulate the glutamate content of filled vesicles.

Received April 18, 2006; revised Sept. 20, 2006; accepted Sept. 22, 2006.

This work was supported by National Institutes of Health Grant DC04055.

Correspondence should be addressed to Laurence O. Trussell, Oregon Hearing Research Center, Vollum Institute, Oregon Health and Science University, Mail Code L-335A, 3181 Southwest Sam Jackson Park Road, Portland, OR 97239. E-mail: trussell@ohsu.edu.

DOI:10.1523/JNEUROSCI.1660-06.2006

 0270-6474/06/2611432-05$15.00/0

Materials and Methods

Slice preparation. Two-hundred-micrometer-thick coronal slices containing the medial nucleus of the trapezoid body (MNTB) were prepared from postnatal day 9 to 12 (P9–P12) Wistar rats and P8–P25 ICR mice, as described previously (Borst et al., 1995). Slices were cut in ice-cold artificial CSF (ACSF) ["slicing" ACSF was composed of the following (in mM): 125 NaCl, 2.5 KCl, 25 glucose, 25 $NaHCO_3$, 1.25 NaH_2PO_4, 0.4 ascorbic acid, 3 3-myo-inositol, 2 Na pyruvate, 3 MgCl, 0.1 CaCl] and transferred to a chamber containing "recording" ACSF (composition was the same as slicing ACSF, except $CaCl_2$ and $MgCl_2$ were changed to 2 and 1 mM, respectively) and incubated at 37°C for 30–60 min and thereafter at room temperature. Two-hundred-micrometer-thick slices containing anteroventral cochlear nuclei (AVCN) were prepared in the same manner.

Recordings. Slices were transferred to a chamber and perfused with recording ACSF. For the perforated-patch recordings, the ACSF was heated to 31–33°C. Slices were viewed using infrared differential interference contrast optics and a 63× water immersion lens. Open-tip resistances were 2–3 MΩ for postsynaptic electrodes, 3–4 MΩ for presynaptic electrodes in young animals, and 6–8 MΩ for presynaptic electrodes in older mice. Recordings were made using an Axopatch 200B amplifier (Molecular Devices, Sunnyvale, CA).

Perforated-patch recordings. For most perforated-patch recordings, we used a KCl-based pipette solution [composed of the following (in mM): 150 KCl, 10 HEPES, 2 MgATP, 10 Na_2-phosphocreatine, 5 EGTA]. In some cases, KCl was substituted for K-gluconate, CsCl, or Cs-methanesulphonate, as indicated. Gramicidin was dissolved in DMSO at 20 mg/ml and added to the pipette solution to make a final concentration of 20–60 μg/ml. The electrode tip was filled with gramicidin-free solution and the barrel with gramicidin-containing solution. For presynaptic recordings, 200 μM Lucifer yellow was added to the pipette solution to ensure that the patch had not ruptured during the recording and to

confirm that the recording was presynaptic by rupturing the patch at the end.

After sealing, series resistance was monitored with 5 mV hyperpolarizing pulses. It typically took 20–30 min for the series resistance (R_S) to drop to <70 MΩ and stabilize (usually to ~50 MΩ but sometimes as low as 30 MΩ).

Glycine (1 mM) was dissolved in recording ACSF and pressure ejected from a patch-type electrode. The pipette was positioned ~20 μm from the cell or calyx, but the exact position and the duration of glycine application (200–500 ms) was adjusted to give the largest response. Calyces or cells were stepped to various potentials for 2 s before glycine application. We allowed at least 30 s between applications. Signals were filtered at 1 kHz and sampled at 10 kHz. R_S was regularly monitored during recording by applying a −5 mV step and measuring the instantaneous peak amplitude of the current transient, filtered at 10 kHz and sampled at 50 kHz. When analyzed, the holding potentials were corrected for the voltage drop across this resistance.

Paired recordings. For paired recordings, the solution in the postsynaptic electrode contained the following (in mM): 75 KCl, 75 K-gluconate, 10 Na_2-phosphocreatine, 10 HEPES, 5 EGTA, 2 MgATP. For the presynaptic electrode, the 100 mM Cl^- solution contained the following (in mM): 100 KCl, 50 K-gluconate, 10 Na_2-phosphocreatine, 10 HEPES, 0.5 EGTA, 2 MgATP, 1 glutamate. For recordings in 10 and 5 mM Cl^-, the appropriate amount of KCl was replaced with K-gluconate.

mEPSCs were recorded in the ACSF with TTX (0.5 μM), strychnine (2 μM), and gabazine (10 μM). Signals were filtered at 5 kHz and sampled at 20 kHz. mEPSCs were detected using a sliding template algorithm. For each recording, a mEPSC was selected visually as a template. The fit was adjusted so that when judged visually, 10–20% of the events detected were deemed spurious and rejected, and no obvious mEPSCs went undetected.

Drugs. Except for glycine, all drugs were bath applied. Most were stored as aqueous solutions at 1000× the final concentration. 4-Aminopyridine and bumetanide were dissolved in DMSO at 1000× the final concentration. Furosemide was dissolved to 100× the final concentration in a solution of 500 μM NaOH. In recordings including K^+ channel blockers, 20 mM NaCl in the ACSF was substituted for 20 mM tetraethylammonium (TEA).

Data analysis. Data were analyzed using Clampfit9.2 (Molecular Devices). Comparisons between multiple groups were made with one-way ANOVA and Dunnett's test using KyPlot (KyensLab, Tokyo, Japan). Kolmogorov-Smirnoff tests were performed with this software. Data are expressed as ± SEM.

Reversal potential and ion concentration. The $[Cl^-]_i$ was calculated from the Cl^- reversal potential using the Nernst equation, $[Cl]_i = [Cl]_o e^{EglyF/RT}$, where $[Cl]_i$ is the intracellular chloride concentration, $[Cl]_o$ is the extracellular chloride concentration, Egly is the reversal potential of the glycine-evoked current, F is the Faraday constant, R is the gas constant, and T is the temperature. The Goldman–Hodgkin–Katz equation was used to estimate $[Cl^-]_i$ with a finite bicarbonate permeability, $[Cl]_i = (P_{Cl}[Cl]_o/P_{HCO3}[HCO_3]_i) e^{EglyF/RT}$, where P_{Cl} and P_{HCO3} are the relative permeabilities of Cl^- and HCO_3, respectively.

Liquid junction potentials and patch potentials. Corrections were made for liquid junction potentials, which were measured as follows (in mV): −3.9 KCl, −6.7 Cs-methanesulphonate, −2.4 CsCl, and −7.5 KCl/K-gluconate. An additional correction was made for a potential across the perforated patch, between +2 and +4 mV, measured by double-patching a cell with one electrode in the whole-cell recording mode and the other in perforated-patch configuration (Y. Kim, unpublished observations).

Results

Reversal potential of glycine responses

Calyces from young rats (P9–P12) were recorded in the gramicidin perforated-patch configuration and clamped between −75 and −80 mV. The resting membrane potential (V_M at zero holding current) was −77 ± 1.8 mV (n = 7), similar to previously reported values (Borst and Sakmann, 1995). The voltage was then stepped to various holding potentials during which time brief (200–500 ms) puffs of glycine (1 mM) were applied (Fig. 1*A*). Glycine application generated inward currents which varied in amplitude with holding potential (Fig. 1*A*,*D*). The reversal potential (E_{REV}) was obtained by fitting a straight line to the data points in the current–voltage (I–V) curve for each cell and extrapolating to zero current (Fig. 1*B*). This procedure gave a mean E_{REV} of −51 ± 1.6 mV (n = 6). This value was insensitive to small variations in holding potential, as calyces held at −90 mV had similar E_{REV} (−51 ± 2.1 mV; n = 4; $p > 0.05$; one-way ANOVA). This suggests that calyces have a minimal resting Cl^- permeability at these negative potentials.

As an additional check for linearity of the I–V relationship, current amplitudes were normalized for each calyx to the current recorded at or near −70 mV (−70 to −73 mV). The results (Fig. 1*C*) (r = 0.99) confirmed the linearity of the I–V relationship and the accuracy of the voltage clamp up to at least −50 mV. Additional confirmation that the glycine I–V is linear was obtained from recordings with a Cs-based solution (see below).

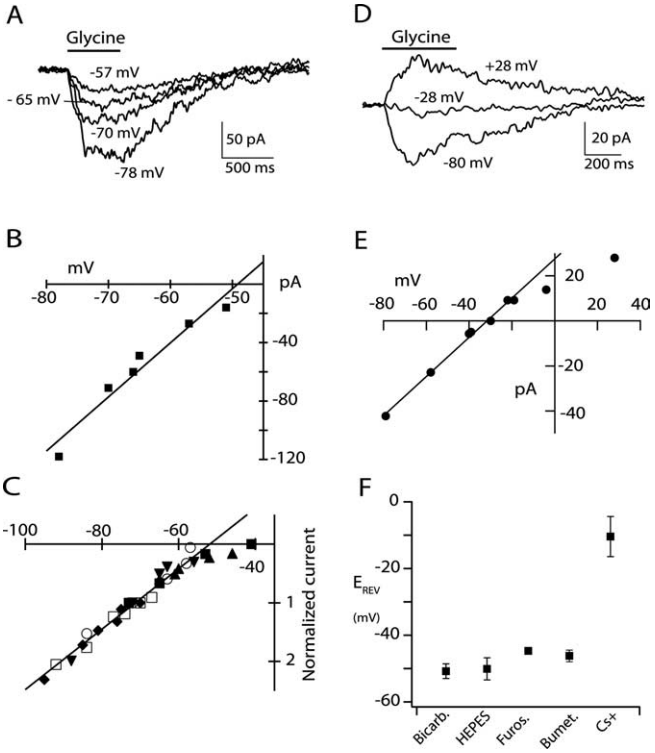

Figure 1. Glycine responses in calyces. ***A***, Glycine-evoked depolarizing currents recorded from a calyx with a K-based pipette solution. One millimolar glycine was puffed for 500 ms with the calyx clamped at the holding potentials indicated. Currents were digitally filtered at 25 Hz. For clarity, only four of the currents are displayed. ***B***, Current–voltage curve for the recordings shown in ***A***. The data points were fitted with a straight line extrapolated to a reversal potential of −49 mV. ***C***, Normalized current–voltage curve for six calyces. Currents were normalized to the current recorded at or near −70 mV. The data were fit with a straight line that excluded the two data points at voltages positive to −50 mV. The extrapolated E_{REV} was −52 mV. ***D***, Glycine-evoked currents recorded from a calyx with a Cs-based intracellular solution, TEA (20 mM), and 4-AP (100 μM) in the ACSF. One millimolar glycine was puffed for 400 ms with the calyx clamped at the holding potentials indicated. ***E***, I–V curve from the calyx shown in ***D***. Note that the I–V curve is linear between −80 and −20 mV, confirming that it is correct to fit a straight line to the data in ***B*** and ***C***. ***F***, Summary of the reversal potential of the glycine-evoked currents under five different recording conditions, which are as follows: bicarbonate-based ACSF, HEPES-based ACSF, with 600 μM furosemide, 30 μM bumetanide, and a Cs-based intracellular solution. The only significant difference in the E_{REV} was with the Cs-based solution.

Calyces have large outward K^+ currents (Ishikawa et al., 2003) that presumably limited how positive we could clamp the membrane potential through the high R_S of the perforated patch. Including the K^+ channel blockers TEA (20 mM) and 4-AP (100 μM), in the ACSF was insufficient to permit reversal of the currents and did not affect the extrapolated E_{REV} (-47 ± 1 mV; $n = 3$). We also examined E_{REV} in mouse MNTB, because calyces are easier to visualize in older animals and therefore more easily studied. In P8–P9 mice, the mean E_{REV} was -37 ± 6 mV ($n = 3$). Responses to glycine were still depolarizing in mice aged P17 ($n = 2$) and P23–P25 ($n = 4$). In the latter group, E_{REV} was -45 ± 6 mV ($n = 3$). Moreover, in several of the mouse calyces, reversal of the currents was apparent.

Using the E_{REV} measured in ACSF, $[Cl^-]$ was calculated as 21 ± 2 mM (see Materials and Methods). Because glycine receptors are permeable to HCO_3^- (Bormann et al., 1987), we assessed their contribution to the glycine-evoked currents by repeating the experiments in a bicarbonate-free, HEPES-buffered ACSF. E_{REV} was not significantly different from that recorded in bicarbonate ACSF (-51 ± 3 mV; $n = 4$; $p > 0.05$; one-way ANOVA) (Fig. 1*F*), suggesting negligible contribution from HCO_3^-. However, because cells continually produce bicarbonate, even in a HEPES-buffered ACSF, we also calculated $[Cl^-]$ assuming an $[HCO_3^-]_i$ of 15 mM (Deitmer and Rose, 1996) and a permeability ratio P_{Cl}:P_{HCO3} of 10:1 (Bormann et al., 1987) (see Materials and Methods), yielding a value of 15 ± 2 mM.

In immature neurons, Cl^- is accumulated in the soma by the Na/K/2Cl transporter NKCC1 (Payne et al., 2003). To test whether this transporter is responsible for the high $[Cl^-]_i$ in the calyx, we preincubated slices for ≥30 min with 30 μM bumetanide, a blocker of NKCC1 (Isenring et al., 1998); bumetanide was also present during the recordings. To ensure that $[Cl^-]_i$ had a chance to decrease, glycine was puffed intermittently while waiting for perforation. Nevertheless, there was no difference in E_{REV} (-46 ± 1.3 mV; $n = 4$; $p > 0.05$; one-way ANOVA) (Fig. 1*F*). We also preincubated and recorded with a high concentration of furosemide (600 μM), which also blocks NKCC1 (Gillen et al., 1996); this also had no affect on the E_{REV} (-45 ± 0.4 mV; $n = 3$) (Fig. 1*F*). However, as shown in Figure 1*D–F*, after replacing intraterminal K^+ using a CsCl- or Cs-methanesulphonate-based intracellular solution, currents reversed significantly more positive than with K-based solutions, at -10 ± 6 mV ($n = 9$; $p < 0.001$; one-way ANOVA). In six of these recordings, the ACSF contained TEA (20 mM), 4-AP (100 μM), and Cs (1 mM) and in three, these drugs were omitted, but in both cases there was a similar positive shift in the reversal potential ($p = 0.6$, unpaired *t* test). Thus, K^+-dependent Cl^- transport may be required for maintenance of E_{REV}.

Somatic versus presynaptic Cl^- regulation

Calyces are the terminals of globular bushy cells in the AVCN. To determine whether these cells can differentially regulate $[Cl^-]_i$ in their somas and terminals, we made perforated-patch recordings from somas of AVCN neurons in young rats (P9–P11) and recorded glycine-evoked responses. Globular bushy cells were identified by their location and their firing patterns in current clamp (Wu and Oertel, 1984) (Fig. 2*A*). Cells were clamped at -60 mV and stepped briefly to different membrane potentials while 1 mM glycine was applied (500 ms puff). All cell bodies responded to glycine with outward currents at a holding potential of -60 mV. Based on their firing pattern, 11 of 22 cells were classified as globular bushy cells. In these, E_{REV} (-94 ± 5mV) (Fig. 2*B–D*) significantly hyperpolarized to the resting membrane potential (measured in current clamp) of -68 ± 6 mV ($p < 0.001$; paired *t* test.). Assuming $[HCO_3]_i$ of 15 mM, this potential corresponds to $[Cl^-]_i$ of 3.8 ± 0.7 mM. These data demonstrate that axon terminals maintain Cl^- at a markedly higher level than in their parent cell bodies.

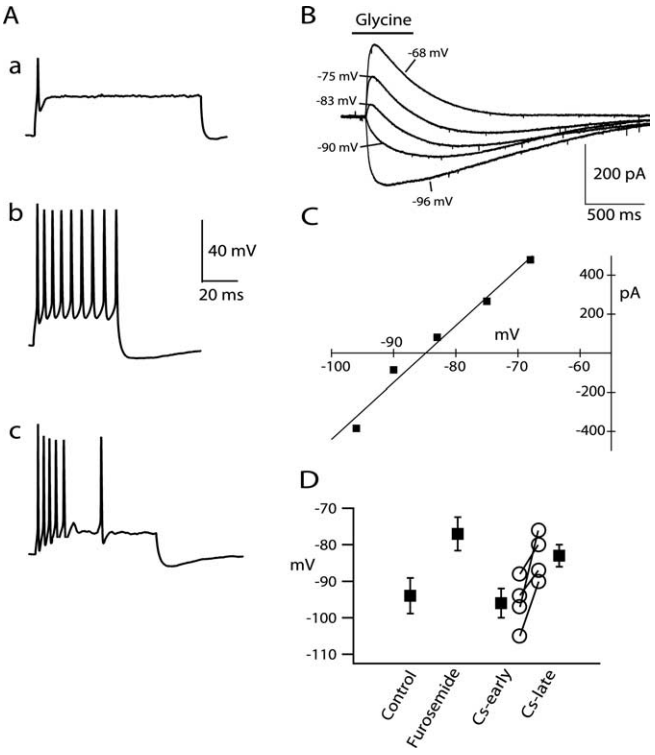

Figure 2. Somatic glycine responses. ***A***, Typical examples of the three different firing patterns of AVCN cells in current-clamp mode in response to current injections. ***a***, A cell firing a single action potential that failed to overshoot 0 mV, at the start of a 100 ms, 450 pA pulse, characteristic of a bushy cell. ***b***, A cell firing action potentials regularly throughout the 100 pA, 50 ms pulse, characteristic of a stellate cell. ***c***, A cell with an irregular firing pattern during the 200 pA, 100 ms pulse; this may be an immature stellate cell. ***B***, Glycine-evoked currents from the bushy cell in ***A***. The cell was held at the holding potentials shown on the left and 1 mM glycine puffed for 500 ms. Note the biphasic response to glycine, seen most clearly at -83 mV. The first phase is predominantly a Cl^- current, whereas the second phase may be dependent on bicarbonate and external K^+ (Staley et al., 1995; Kaila et al., 1997). ***C***, *I–V* curve for the early response of the cell shown in ***B***. For -90 mV and -96 mV, the current amplitude was measured at the same time as the peak outward current measured at -83 mV. The reversal potential was -86 mV, considerably more negative than the resting membrane potential of -62 mV. ***D***, Summary of the E_{REV} of glycine-evoked currents under different recording conditions. Left, K-based internal solution; middle, K-based solution plus furosemide; right, shift in E_{REV} with a Cs-based recording solution over a 10–20 min period. Lines connect data from early and late in the recording, as Cs^+ entered the cell.

Chloride is commonly extruded from neurons by the furosemide-sensitive K^+/Cl^- exchanger, KCC2. In slices preincubated with furosemide (600 μM) ($n = 5$), E_{REV} in bushy cells was 17 mV more positive than in control slices (Fig. 2*D*) (-77 ± 4.6 mV vs -94 ± 4.9 mV; $p = 0.007$; unpaired *t* test). When intracellular K was replaced using a CsCl-based pipette solution and the cell clamped at -60 mV, there was a gradual positive shift in E_{REV} during the recording of 7–21 mV (Fig. 2*D*) (mean shift, 12 ± 4 mV; $n = 4$; $p = 0.03$; paired *t* test), probably reflecting slow diffusion of Cs^+ through the perforated patch. This inference is supported by the observation that the resting potential, measured by briefly switching to current clamp, shifted positive by 6–10 mV over the same time course.

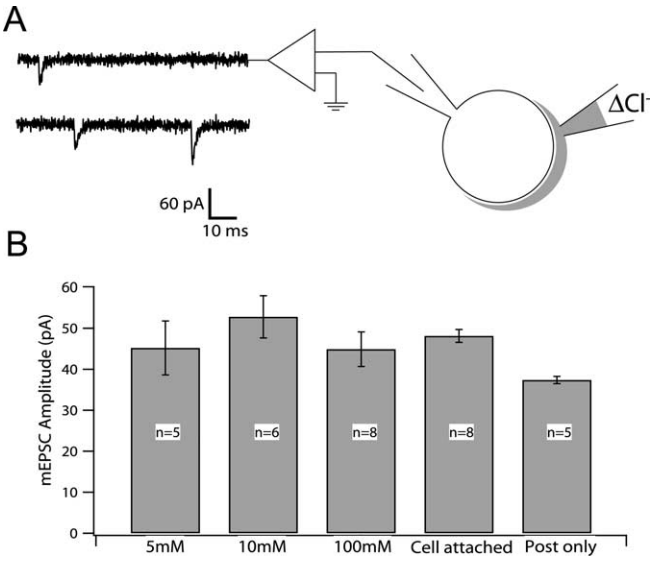

Figure 3. Presynaptic Cl^- concentration does not affect the amplitude of glutamatergic mEPSCs. ***A***, Right, Diagram of the recording configuration. Spontaneous glutamatergic mEPSCs (left) were recorded from the postsynaptic cell. The presynaptic electrode contained either 5, 10, or 100 mM Cl^-. TTX (0.5 μM), strychnine (2 μM), and gabazine (10 μM) were included in the ACSF. The mEPSCs shown here were recorded with 5 mM Cl^- in the presynaptic electrode. ***B***, Average amplitude of glutamate mEPSCs recorded after 3 min in different concentrations of presynaptic Cl^-. There was no difference in amplitude in different Cl^- concentrations or with a cell-attached electrode. Amplitudes were as follows: 5 mM, 45 $\pm$ 6.6 pA, $n = 6$; 10 mM, 53 $\pm$ 5.1 pA, $n = 5$; 100 mM, 45 $\pm$ 4.2 pA, $n = 8$; cell attached, 48 $\pm$ 1.6 pA, $n = 8$; $p = 0.56$; one-way ANOVA). mEPSCs were significantly smaller when recordings were made from the postsynaptic cell alone.

Stability of vesicular glutamate content

We could test the effect of $[Cl^-]_i$ on vesicle content because glutamate receptors are not saturated by a single quantum of transmitter and increased vesicle filling can be detected as an increase in mEPSC amplitude (Ishikawa et al., 2002). We made paired whole-cell presynaptic and postsynaptic recordings in which presynaptic $[Cl^-]$ was varied. Glutamatergic mEPSCs were recorded with TTX (0.5 μM), strychnine (2 μM), and gabazine (10 μM) in the ACSF (Fig. 3*A*). After establishing presynaptic recording, we waited ~3 min to complete dialysis of the terminal with the pipette solution before recording mEPSCs. There was no difference in mEPSC amplitudes recorded with the three different $[Cl^-]$ or with a cell-attached electrode (Fig. 3*B*). Most paired recordings lasted only a few minutes, just long enough to record sufficient mEPSCs for analysis. We were concerned that re-equilibration of the vesicle contents might require more time. However, in some experiments, we were able to hold pairs long enough to examine how the mEPSC amplitude varied over time. With 100 mM presynaptic chloride, three of six cells had stable mEPSC amplitudes up to 25 min post-break-in; in the three cells where there was a detectable decrease, mean mESPC amplitudes were still in excess of 30 pA 8–20 min after break-in. For comparison, in 5 and 10 mM $[Cl^-]_i$, two of four and three of four cells, respectively, had stable mEPSC amplitudes over similar time spans. Therefore, in contrast to the prediction from biochemical experiments, high $[Cl^-]_i$ did not significantly alter vesicular glutamate content *in situ*, at least over a 25 min period.

Discussion

The calyx of Held acts as an autonomous neuronal compartment with respect to handling Cl^-, maintaining a concentration five-times higher than in the soma. Unlike the soma of many neurons, the concentration remains elevated in the calyx in animals older than 3 weeks. Because most developmental changes in the calyx are complete by ~P14, a high calyceal $[Cl^-]$ is likely a feature of the adult brain. Neither bumetanide nor furosemide, blockers of the common somatic and dendritic Na^+- and K^+-dependent Cl^- transporters, altered the Cl^- concentration. This contrasts with glutamate terminals in the ventromedial hypothalamus where Cl^- uptake was sensitive to these drugs (Jang et al., 2001), but is consistent with a study in the lateral superior olive, where NKCC1 was not responsible for accumulating Cl^- in neonatal neuronal soma (Balakrishnan et al., 2003). Replacing intracellular K^+ with Cs^+ increased $[Cl^-]_i$, suggesting the disruption of a Cl^- transporter coupled to K^+ transport (Kakazu et al., 2000), although it does not distinguish between alteration of inward- versus outward-directed transport. The possible coexpression of inward- and outward-directed Cl^- transporters potentially allows finer adjustment of $[Cl^-]_i$. Meanwhile, globular bushy cell soma have a Cl^- extrusion mechanism sensitive to intracellular Cs^+ and extracellular furosemide, indicative of the KCC2 transporter. The lack of effect of furosemide on the calyx suggests that functional KCC2 is absent from the terminal.

In vitro experiments described a bell-shaped relationship between $[Cl^-]$ and vesicular glutamate content (Naito and Ueda, 1985; Varoqui et al., 2002). Glutamate is in dynamic equilibrium across the synaptic vesicle (Wang and Floor, 1994), suggesting that brief changes in $[Cl^-]$, as might occur during intense glycinergic signaling, could alter this equilibrium and consequently the quantal amplitude. However, quantal amplitudes were not significantly different between calyces dialyzed for 3 min with $[Cl^-]$ of 5, 10, and 100 mM, concentrations over which vesicular glutamate accumulation *in vitro* varies greatly. In 100 mM Cl^-, vesicular glutamate uptake is as little as 15–20% of maximum (Naito and Ueda, 1985) and is absent at 150 mM (Varoqui et al., 2002). In contrast, we typically measured stable quantal amplitudes for as long as 25 min in 100 mM Cl^-. The rate of glutamate efflux in an intact terminal is unknown. Although a relatively slow efflux would retain glutamate in 100 mM Cl^-, it would also favor additional glutamate accumulation in 5 mM Cl^-, which we did not detect. The reverse argument is also true. Thus, brief changes in terminal $[Cl^-]$ are not translated into changes in quantal amplitude. Additional experiments are needed to determine the effect of terminal $[Cl^-]$ on filling of new vesicles.

Our estimate of 21 mM for $[Cl^-]_i$ is similar to estimates in pituitary terminals (20 mM) (Zhang and Jackson, 1995) and retinal bipolar cell terminals (22 mM) (Billups and Attwell, 2002). Elevated $[Cl^-]_i$ is necessary for the depolarizing action of glycine or GABA. Furthermore, different lines of evidence suggest that the amount of depolarization determines whether transmitter release is facilitated or inhibited. First, in primary afferents, reducing depolarization with low concentrations of bicuculline facilitated rather than inhibited glutamate release (Duchen, 1986). Second, in paired recordings, small depolarizations of the calyx facilitated release, but depolarizations positive to -60 mV produced varied effects, sometimes causing inhibition (Awatramani et al., 2005). Facilitation is caused by the weak activation of voltage-gated Ca^{2+} channels and the subsequent small basal Ca^{2+} increase (Awatramani et al., 2005); larger depolarizations inhibit release by inactivating Na^+ and possibly Ca^{2+} channels (Graham and Redman, 1994; Zhang and Jackson, 1995); in some systems the shunting of the action potential by the Cl^- conductance is the primary mechanism of inhibition (Cattaert and El Manira, 1999). In the calyx, K^+ conductances limit slow depolarizations from reaching the Cl^- reversal potential. Further-

more, E_{REV} is similar in the calyx, where release is facilitated, and pituitary neuroendocrine terminals, where it is inhibited (Saridaki et al., 1989). Although elevated $[Cl^-]$ is necessary for these effects, clearly the Cl^- reversal potential per se does not determine how transmitter release is modulated. The fact that three anatomically and functionally distinct terminals, the calyx of Held, retinal bipolar terminals, and pituitary neuroendocrine terminals, maintain a similar $[Cl^-]$ suggests that other aspects of presynaptic physiology contribute to determining the functional role of Cl^- in the regulation of synaptic strength.

References

Alvarez-Leefmans FJ, Gamino SM, Giraldez F, Nogueron I (1988) Intracellular chloride regulation in amphibian dorsal root ganglion neurones studied with ion-selective microelectrodes. J Physiol (Lond) 406:225–246.

Awatramani GB, Price GD, Trussell LO (2005) Modulation of transmitter release by presynaptic resting potential and background calcium levels. Neuron 48:109–121.

Balakrishnan V, Becker M, Lohrke S, Nothwang HG, Guresir E, Friauf E (2003) Expression and function of chloride transporters during development of inhibitory neurotransmission in the auditory brainstem. J Neurosci 23:4134–4145.

Billups D, Attwell D (2002) Control of intracellular chloride concentration and GABA response polarity in rat retinal ON-bipolar cells. J Physiol (Lond) 545:183–198.

Bormann J, Hamill OP, Sakmann B (1987) Mechanism of anion permeation through channels gated by glycine and gamma-aminobutyric acid in mouse cultured spinal neurones. J Physiol (Lond) 385:243–286.

Borst JG, Helmchen F, Sakmann B (1995) Pre- and postsynaptic whole-cell recordings in the medial nucleus of the trapezoid body of the rat. J Physiol (Lond) 489:825–840.

Cattaert D, El Manira A (1999) Shunting versus inactivation: analysis of presynaptic inhibitory mechanisms in primary afferents of the crayfish. J Neurosci 19:6079–6089.

Deitmer JW, Rose CR (1996) pH regulation and proton signalling by glial cells. Prog Neurobiol 48:73–103.

Duchen MR (1986) Excitation of mouse motoneurones by GABA-mediated primary afferent depolarization. Brain Res 379:182–187.

Duebel J, Haverkamp S, Schleich W, Feng G, Augustine GJ, Kuner T, Euler T (2006) Two-photon imaging reveals somatodendritic chloride gradient in retinal ON-type bipolar cells expressing the biosensor clomeleon. Neuron 49:81–94.

Gillen CM, Brill S, Payne JA, Forbush B (1996) Molecular cloning and functional expression of the K-Cl cotransporter from rabbit, rat, and human. A new member of the cation-chloride cotransporter family. J Biol Chem 271:16237–16244.

Graham B, Redman S (1994) A simulation of action potentials in synaptic boutons during presynaptic inhibition. J Neurophysiol 71:538–549.

Hull C, von Gersdorff H (2004) Fast endocytosis is inhibited by GABA-mediated chloride influx at a presynaptic terminal. Neuron 44:469–482.

Isenring P, Jacoby SC, Payne JA, Forbush III B (1998) Comparison of Na-K-Cl cotransporters. NKCC1, NKCC2, and the HEK cell Na-L-Cl cotransporter. J Biol Chem 273:11295–11301.

Ishikawa T, Sahara Y, Takahashi T (2002) A single packet of transmitter does not saturate postsynaptic glutamate receptors. Neuron 34:613–621.

Ishikawa T, Nakamura Y, Saitoh N, Li WB, Iwasaki S, Takahashi T (2003) Distinct roles of Kv1 and Kv3 potassium channels at the calyx of Held presynaptic terminal. J Neurosci 23:10445–10453.

Jang IS, Jeong HJ, Akaike N (2001) Contribution of the Na-K-Cl cotransporter on $GABA_A$-receptor-mediated presynaptic depolarization in excitatory nerve terminals. J Neurosci 21:5962–5972.

Jang IS, Nakamura M, Ito Y, Akaike N (2006) Presynaptic GABA(A) receptors facilitate spontaneous glutamate release from presynaptic terminals on mechanically dissociated rat CA3 pyramidal neurons. Neuroscience 138:25–35.

Kaila K, Lamsa K, Smirnov S, Taira T, Viopio J (1997) Long-lasting GABA-mediated depolarization evoked by high-frequency stimulation in pyramidal neurons of rat hippocampal slice is attributable to a network-driven, bicarbonate-dependent K^+ transient. J Neurosci 17:7662–7672.

Kakazu Y, Uchida S, Nakagawa T, Akaike N, Nabekura J (2000) Reversibility and cation selectivity of the K(+)-Cl(−) cotransport in rat central neurons. J Neurophysiol 84:281–288.

Naito S, Ueda T (1985) Characterization of glutamate uptake into synaptic vesicles. J Neurochem 44:99–109.

Nishi S, Minota S, Karczmar AG (1974) Primary afferent neurones: the ionic mechanism of GABA-mediated depolarization. Neuropharmacology 13:215–219.

Payne JA, Rivera C, Voipio J, Kaila K (2003) Cation-chloride cotransporters in neuronal communication, development and trauma. Trends Neurosci 26:199–206.

Rudomin P, Schmidt RF (1999) Presynaptic inhibition in the vertebrate spinal cord revisited. Exp Brain Res 129:1–37.

Saridaki E, Carter DA, Lightman SL (1989) γ-Aminobutyric acid regulation of neurohypophysial hormone secretion in male and female rats. J Endocrinol 121:343–349.

Staley KJ, Soldo BL, Proctor WR (1995) Ionic mechanisms of neuronal excitation by inhibitory $GABA_A$ receptors. Science 269:977–981.

Tabb JS, Kish PE, Van Dyke R, Ueda T (1992) Glutamate transport into synaptic vesicles. Roles of membrane potential, pH gradient, and intravesicular pH. J Biol Chem 267:15412–15418.

Takamori S, Rhee JS, Rosenmund C, Jahn R (2000) Identification of a vesicular glutamate transporter that defines a glutamatergic phenotype in neurons. Nature 407:189–194.

Turecek R, Trussell LO (2001) Presynaptic glycine receptors enhance transmitter release at a mammalian central synapse. Nature 411:587–590.

Varoqui H, Schafer MK, Zhu H, Weihe E, Erickson JD (2002) Identification of the differentiation-associated Na^+/PI transporter as a novel vesicular glutamate transporter expressed in a distinct set of glutamatergic synapses. J Neurosci 22:142–155.

Wang Y, Floor E (1994) Dynamic storage of glutamate is rat-brain synaptic vesicles. Neurosci Lett 180:175–178.

Wu SH, Oertel D (1984) Intracellular injection with horseradish peroxidase of physiologically characterized stellate and bushy cells in slices of mouse anteroventral cochlear nucleus. J Neurosci 4:1577–1588.

Zhang SJ, Jackson MB (1993) GABA-activated chloride channels in secretory nerve endings. Science 259:531–534.

Zhang SJ, Jackson MB (1995) GABAA receptor activation and the excitability of nerve terminals in the rat posterior pituitary. J Physiol (Lond) 483:583–595.